Microscopic theory of orientational disorder and lattice instability in solid C_{70}

A. K. Callebaut and K. H. Michel
Department of Physics, Universiteit Antwerpen (UIA), B-2610 Antwerpen, Belgium
(Received 13 February 1995; revised manuscript received 31 July 1995)

We have developed a microscopic theory which describes the orientational dynamics of C_{70} molecules and its coupling to lattice displacements in the face-centered-cubic phase of C_{70} fullerite. The single-molecule orientational density distribution in the disordered phase is calculated. The ferroelastic transition to the rhombohedral phase is investigated. The discontinuity of the orientational order parameter at the phase transition is calculated. It is found that the transition leads to a stretching of the primitive unit cell along a [111] cubic direction. A softening of the elastic constant c_{44} at the transition is predicted.

I. INTRODUCTION

Besides solid C_{60}, which is the most prominent molecular crystal of the fullerite series, solid C_{70} has become a subject of intense research.[1–3] In solid C_{60} the transition from the orientationally disordered phase (space group $Fm\bar{3}m$) to the ordered phase (space group $Pa\bar{3}$) is essentially an orientational phenomenon (see, e.g., Refs. 4 and 5). The concomittant contraction of the lattice is a secondary effect, which does not affect the lattice symmetry.

In solid C_{70} the situation is different. Although in early work[1,6] it was found that samples of solid C_{70} contain mixtures of hexagonal and face-centered-cubic (fcc) phases at room temperature (T), it seems by now established that at high T the stable structure has space group $Fm\bar{3}m$ with orientationally disordered molecules.[7,8] With decreasing T a transition to a rhombohedral phase (space groups $R\bar{3}m$) occurs at $T\approx 340$ K, followed by a transition to a monoclinic phase[3,6,8] at still lower T. Such a scenario has been predicted earlier by molecular-dynamics simulations.[2] In accordance with experimental observations,[6,3,8] molecular dynamics shows that in the rhombohedral phase the molecules are on the average oriented along a [111] direction of the former cubic phase and that the unit cell is stretched. Recently the orientational ordering in solid C_{70} has been studied in frame of a Landau free energy, which includes a bilinear coupling of orientational quadrupoles of the T_{2g} symmetry to trigonal shear strains.[9] In particular a condensation of orientations then entails a trigonal deformation of the lattice.

It has been noticed[10] that the sequence of structural phase transitions in C_{70} is in many aspects similar to ferroelastic phase transitions encountered in mixed crystals of alkali-metal halides cyanides.[11–13] There the coupling of orientational modes of T_{2g} symmetry to acoustic lattice displacements[14] [called translation-rotation (T-R) coupling] drives the transition (for a review see Ref. 10). There are two major differences. There are no counterions in solid C_{70}, and the molecule is nonlinear.

In the present paper we will give a microscopic theory of the orientational dynamics of the C_{70} molecules and their coupling to lattice vibrations. We will derive the bilinear T-R rotation coupling from an atomistic model of the intermolecular potential. This coupling gives rise to an effective lattice-mediated interaction between orientational fluctuations of T_{2g} symmetry, which drives the transition to the rhombohedral phase. We study the orientational and the displacive collective susceptibilities and predict a softening of the elastic constants c_{44} near the transition to the rhombohedral phase. We calculate the orientational distribution function in the disordered phase. We determine the discontinuity of the orientational order parameter at the first-order phase transition and find that the trigonal deformation corresponds to a stretching of the unit cell.

II. ORIENTATIONAL COORDINATES AND MOLECULAR STRUCTURE

A convenient way to treat orientation-dependent properties of nonlinear molecules in crystals is to use rotator functions. These functions, introduced by James and Keenan[15] for the description of solid CD_4, are linear combinations of Wigner's D matrices. The rotator functions take into account the symmetry of the molecule and of the site.[16,17] The C_{70} molecule has symmetry D_{5h}.[18] It has been found by inelastic neutron-scattering experiments[7,19] that in the high-temperature phase, the molecule performs fast rotations about its long axis, and effectively behaves as a solid object of $D_{\infty h}$ symmetry. We will take advantage of this fact to simplify considerably the mathematical description.

We start with a molecule in its standard orientation with respect to a rectangular Cartesian coordinate system. The molecule is centered at the origin, its fivefold axis is taken as z axis, the (x,y) plane is a symmetry plane. The Cartesian coordinates of the molecule, taken as a rigid body, are specified in Ref. 18. It is convenient to classify the atoms (also called C centers) of the molecule in (001) planes. We consider five groups of atoms labeled by an index λ: ten atoms in the equatorial plane $z(\lambda=1)=0$, ten atoms in each of the planes $\pm z(\lambda)$, $\lambda=2,3$, and five atoms in each of the planes $\pm z(\lambda)$, $\lambda=4,5$. The atoms are labeled by indices $\nu(\lambda)$, where $\nu=1-10$ or $1-20$. The position of atom $\nu(\lambda)$ is described by the polar coordinates $[d(\lambda), \Omega'(\nu(\lambda))]$ where d measures the distance from the origin to the atom and where $\Omega'=(\theta',\phi')$ stands for the polar angles. In order to account for the molecular symmetry, we calculate the coefficients[20]

$$c_l^m(\lambda)=\sum_{\nu=1}^{n(\lambda)} Y_l^m[\Omega'(\nu(\lambda))]. \tag{2.1}$$

TABLE I. Structural data of model of C_{70} molecule. Coefficients $c_l^0(\lambda)$; rows $\lambda=1$–5 refer to C centers, $\lambda=6,7$ to D centers and $\lambda=8,9$ to I centers. Heights of planes $z(\lambda)$ in units Å; distances $d(\lambda)$ from center of mass of molecule to interaction center in plane $\pm z(\lambda)$ in units Å; $n(\lambda)$ number of centers in group λ, factors 2 denote that there are two planes for the given λ. One has $c_0^0(\lambda)=(1/\sqrt{4\pi})n(\lambda)$.

λ l	2	4	6	8	$z(\lambda)$	$d(\lambda)$	$n(\lambda)$
1	−3.15	3.17	−3.18	3.18	0	3.565	10
2	−4.29	0.41	3.70	−6.28	1.197	3.663	10×2
3	1.25	−7.19	1.80	6.44	2.449	3.876	10×2
4	2.95	−1.89	−4.03	−0.31	3.235	4.029	5×2
5	5.47	5.00	2.48	−0.92	3.983	4.172	5×2
6	4.39	1.40	−2.84	−4.73	3.609	4.043	5×2
7	0.74	−3.62	0.61	3.41	2.449	3.816	5×2
8	−2.10	0.11	1.97	−3.17	1.197	3.593	5×2
9	−5.77	4.60	−2.86	0.79	0.599	3.544	10×2

Here $n(\lambda)$ is the number of atoms in group λ. We use the definition of spherical harmonics of Bradley and Cracknell:[21]

$$Y_l^m(\Omega)=\left(\frac{(2l+1)(l-|m|)!}{4\pi(l+|m|)!}\right)^{1/2}P_l^{|m|}(\cos\theta)e^{im\phi}. \tag{2.2}$$

Symmetry of the molecule implies that the coefficients c_l^m are different from zero for[9,7] $m=0, \pm5,10...$, and l-m even.

Following the model of molecular-dynamics calculations,[2] we do not only consider the atoms as centers of intermolecular interactions but also centers of "double bonds" on the C_{60}-like polar caps of the C_{70} molecule. There are ten of these "D centers" on the short bonds with midpoints in planes $\pm z(6)$, and ten on short bonds with midpoints in planes $\pm z(7)$. Finally we consider interaction centers located on intermediate bonds[2] ("I centers"), five centers in each of the planes $\pm z(8)$, and ten in each of the planes $\pm z(9)$. The coordinates are given in Table I. The distribution of these centers also has symmetry D_{5h}, and hence the corresponding coefficients $c_l^m(\lambda)$ have the same properties as those of the C centers. As we will show in the following, we can restrict ourselves to orientational properties described by functions Y_l^m belonging to the manifolds $l=2$, 4, 6, and 8. We then have

$$c_l^m(\lambda)=c_l^0(\lambda)\delta_{m0}. \tag{2.3}$$

The coefficients $c_l^0(\lambda)$ are quoted in Table I. Since $m=0$, the azimuthal angle ϕ in Eq. (2.2) is irrelevant, the molecule is spinning around its fivefold axis. When the molecule is tilted away from its standard position, its orientation is then specified by the polar angles $\omega\equiv(\beta,\alpha)$ which determine the orientation of the fivefold molecular axis in the crystal fixed frame.

In order to describe orientation dependent properties in the disordered phase, we use site symmetry adapted functions (SAF's)

$$S_{l(O_h)}^{\tau}(\Omega)=\sum_{m=-l}^{l}Y_l^m(\Omega)\alpha_l^{m\tau}. \tag{2.4}$$

Here $\tau=(\Gamma,\rho,\delta)$, where Γ refers to the irreducible representations of the cubic site point group O_h, ρ labels the subspaces if Γ occurs more than once for a given l, δ labels the components of Γ. The coefficients $\alpha_l^{m\tau}$ are tabulated in Ref. 21.

Symmetry implies[22] that the transition from the cubic phase to the rhombohedral phase with site symmetry D_{3d} is driven by fluctuations belonging to the irreducible representation $\Gamma=T_{2g}$ of O_h. The lowest allowed value of l is then 2, and corresponds to orientational quadrupoles of T_{2g} symmetry.[9] Notice that this situation is also familiar from the theoretical description[23] of the phase transition $Fm\bar{3}m\rightarrow R\bar{3}m$ in the mixed-alkali-metal halides cyanides crystals. As we will see each C_{70} molecule in the cubic phase experiences a static crystal field. The corresponding orientational fluctuations belong to the unit representation $\Gamma=A_{1g}$ of O_h. In the following we will then restrict ourselves to SAF's belonging to the manifolds $l=4,6,8$ for the fluctuations of A_{1g} symmetry and to $l=2$ for those of T_{2g} symmetry. The corresponding functions are quoted in Appendix A.

We now want to relate the site symmetry to the molecular symmetry. We consider interaction centers of plane(s) λ and define, for an arbitrary orientation of the molecule, the function

$$\sum_{\nu(\lambda)=1}^{n(\lambda)}S_l^{\tau}[\Omega(\nu(\lambda))]=\sum_{\nu(\lambda)}\sum_{m}\alpha_l^{m\tau}Y_l^m[\Omega(\nu(\lambda))] \equiv U_l^{\tau}(\omega,\lambda). \tag{2.5}$$

Here $\Omega(\nu(\lambda))$ stands for the polar angles of the center $\nu(\lambda)$ if the molecule is tilted away from its standard position by a rotation $R(\omega)$. Denoting again by $\Omega'(\nu(\lambda))$ the corresponding polar coordinates if the molecule is in standard orientation, we have $\Omega(\nu(\lambda))=R(\omega)\Omega'(\nu(\lambda))$. The transformation law for the spherical harmonics reads

$$Y_l^m[\Omega(\nu(\lambda))]=\sum_n D_l^{nm}(\omega)Y_l^n[\Omega'(\nu(\lambda))], \tag{2.6}$$

where $D_l^{nm}(\omega)$ are the Wigner matrices which depend on the Euler angles ω. Inserting Eq. (2.6) into (2.5) and using Eq. (2.3), we obtain the rotator function

$$U_l^{\tau}(\omega,\lambda)=c_l^0(\lambda)\sum_m D_l^{0m}(\omega)\alpha_l^{m\tau}, \tag{2.7}$$

where

$$D_l^{0m}(\omega)=(-1)^m\left(\frac{4\pi}{2l+1}\right)^{1/2}Y_l^m(\beta,\alpha)^*. \quad (2.8)$$

We recall that β and α are the polar and azimuthal angles of the fivefold axis. We see that the molecule effectively behaves as a dumbbell of symmetry $D_{\infty h}$. However we should keep in mind that the molecule is a nonlinear object, and that the three-dimensional shape of the molecule is accounted for by the coefficients $c_l^0(\lambda)$. They play a role of structure constants of the molecule. This point will become more evident in the next section where we study the intermolecular potential.

III. ORIENTATION AND TRANSLATION-DEPENDENT INTERACTIONS

In this section we derive the interaction potential between rotating molecules on a deformable lattice. Our calculation will be microscopic in as far as it starts from the interactions between centers on different molecules, however the form and the strength of the interaction between centers is based on phenomenological assumptions.

We consider a crystal of N molecules C_{70} in the cubic phase. The center of mass positions of the molecules occupy an fcc lattice. The lattice sites are labeled by an index $\vec{n}$, the center-of-mass positions in a deformable lattice are given by

$$\vec{R}(\vec{n})=\vec{X}(\vec{n})+\vec{s}(\vec{n}), \quad (3.1)$$

where $\vec{X}(\vec{n})$ is the rigid-lattice position and $\vec{s}(\vec{n})$ the instantaneous lattice displacement. The position of the interaction center $\nu(\lambda)$ in the $\vec{n}$th molecule is then given by

$$\vec{R}(\vec{n},\lambda,\nu)=\vec{R}(\vec{n})+\vec{d}(\nu(\vec{n},\lambda)). \quad (3.2)$$

Here $\vec{d}(\nu(\vec{n},\lambda))$ has polar coordinates $d(\lambda),\Omega(\nu(\vec{n},\lambda))$ and depends on the molecular orientation at site $\vec{n}$. The total intermolecular potential energy is written as a sum of potentials between interaction centers belonging to different molecules

$$V=\frac{1}{2}\sum_{\vec{n}\vec{n}'}\sum_{\lambda\lambda'}\sum_{\nu\nu'}V(\vec{n},\lambda,\nu;\vec{n}',\lambda',\nu'). \quad (3.3)$$

The potential $V(\vec{n},\lambda,\nu;\vec{n}',\lambda',\nu')$ depends on the distance r between the center $\nu(\lambda)$ on molecule $\vec{n}$ and the center $\nu'(\lambda')$ on molecule $\vec{n}'$. One has

$$r=|\vec{R}(\vec{n},\lambda,\nu)-\vec{R}(\vec{n}',\lambda',\nu')|. \quad (3.4)$$

Additional details about the potential will be given in Sec. V where we discuss numerical results. Here it is sufficient to realize that r depends on the instantaneous center-of-mass displacements and on the orientations of the molecules.

We expand the potential in terms of displacements and subsequently in terms of rotator functions and obtain[17]

$$V=V^{RR}+V^{R}+V^{TR}+V^{TT}. \quad (3.5)$$

Here the superscript R refers to rotational coordinates and T to displacements. In particular V^{RR} is the direct orientation-orientation interaction between pairs of molecules on a rigid lattice. We restrict ourselves to interacting orientational modes of T_{2g} symmetry belonging to the manifold $l=2$, i.e., quadrupoles. We have also calculated the interaction of orientational modes of T_{2g} symmetry belonging to the manifold $l=4$ (hexadecapoles) and found that it is more than one order of magnitude smaller. Following the procedure of Ref. 17 for each group of interaction centers λ, we carry out a double expansion of (3.3) in terms of rotator functions (2.7) and obtain

$$V^{RR}=\frac{1}{2}\sum_{\vec{n}\vec{n}'}\mathscr{V}_{\lambda\lambda'}^{\alpha\beta}(\vec{n}-\vec{n}')U_2^{\alpha}(\vec{n},\lambda)U_2^{\beta}(\vec{n}',\lambda'). \quad (3.6)$$

Here we sum over repeated indices α, β, and λ, λ'. The index α refers to the three components of T_{2g} symmetry, we have written U_2^{α} for $U_2^{T_{2g},\alpha}$. We recall that the argument $\vec{n}$ of $U_l^{\alpha}(\vec{n},\lambda)$ stands for $\omega(\vec{n})$ which specifies the instantaneous orientation of the long axis of the molecule at site $\vec{n}$. The expansion coefficients are given by

$$\mathscr{V}_{\lambda\lambda'}^{\alpha\beta}(\vec{n}-\vec{n}')=\int d\Omega_{\nu}\int d\Omega_{\nu'}V(\vec{n},\lambda,\nu;\vec{n}',\lambda',\nu')\times S_2^{\alpha}(\Omega_{\nu})S_2^{\beta}(\Omega_{\nu'}). \quad (3.7)$$

Here S_2^{α} are site symmetry adapted functions belonging to the irreducible representation T_{2g} of O_h. Since the functions $U_l^{\tau}(\vec{n},\lambda)$ occur always in conjunction with the molecular structure coefficients $c_l^0(\lambda)$ [see Eq. (2.7)], it is convenient to consider rotator functions which are independent of the interaction centers λ and to define

$$U_l^{\tau}(\omega)=\sum_m D_l^{0m}(\omega)\alpha_l^{m\tau}, \quad (3.8)$$

while the coefficients $c_l^0(\lambda)$ are counted with the expansion coefficients.

Explicit expressions of rotator functions are given in Appendix A. Defining the molecular interaction coefficient

$$J^{\alpha\beta}(\vec{n}-\vec{n}')=\sum_{\lambda\lambda'}\mathscr{V}_{\lambda\lambda'}^{\alpha\beta}(\vec{n}-\vec{n}')c_2^0(\lambda)c_2^0(\lambda'), \quad (3.9a)$$

we obtain for the potential (3.6)

$$V^{RR}=\frac{1}{2}\sum_{\vec{n}\vec{n}'}J^{\alpha\beta}(\vec{n}-\vec{n}')U_2^{\alpha}(\vec{n})U_2^{\beta}(\vec{n}'). \quad (3.9b)$$

The form of expression (3.9a) is very suggestive. The factor $\mathscr{V}_{\lambda\lambda'}^{\alpha\beta}(\vec{n}-\vec{n}')$ accounts for the strength of the interaction between centers λ and λ' while $c_l^0(\lambda)$ and $c_l^0(\lambda')$ accounts for the density of these centers.

The second term on the right-hand side of Eq. (3.5) is the crystal field in a rigid lattice. This field is experienced by a given molecule when its neighbors are taken in spherical approximation. It can therefore be considered as a special case of V^{RR} where, in a cubic lattice, the central molecule is described by rotator functions of A_{1g} symmetry belonging to the manifold $l=4,6,8...$, while the surrounding molecules are described by rotator functions with $l=0$. From Eqs. (3.8) and (2.8) it follows that $U_{l=0}^{A_{1g}}=1$. We then obtain for the crystal field

$$V^{R}=\sum_l\sum_n w_l^{A_{1g}}U_l^{1A_{1g}}(\vec{n}). \quad (3.10)$$

Restricting ourselves to the 12 nearest neighbors in the fcc lattice, we have

$$w_l^{A_{1g}} = 12 \sum_{\lambda\lambda'} c_0^0(\lambda) c_l^0(\lambda') \mathscr{V}_l^{A_{1g}}(\lambda,\lambda') \tag{3.11}$$

with

$$\mathscr{V}_l^{A_{1g}}(\lambda,\lambda') = \frac{1}{\sqrt{4\pi}} \int d\Omega_\nu d\Omega_{\nu'} V(\vec{n},\lambda,\nu;\vec{n}',\lambda',\nu') \times S_l^{A_{1g}}(\Omega_\nu). \tag{3.12}$$

Here the lattice site $\vec{n}'$ refers to a nearest-neighbor site of $\vec{n}$. Notice that Eq. (3.12) can be considered as a special case of Eq. (3.6), where now the SAF at site $\vec{n}$ has A_{1g} symmetry and belongs to the manifold $l=4$, 6 or 8, while the SAF at $\vec{n}'$ is given by $S_{l=0}^{A_{1g}} = 1/\sqrt{4\pi}$. We also see that expression (3.11) is the crystal-field analogon of the R-R interaction (3.9a). The translation-rotation coupling potential in Eq. (3.5) is given by

$$V^{TR} = \sum_{\vec{n}\vec{n}'} \mathscr{V}_{\alpha i}(\vec{n}'-\vec{n})[s_i(\vec{n}) - s_i(\vec{n}')] U_2^\alpha(\vec{n}), \tag{3.13}$$

where

$$\mathscr{V}_{\alpha i}(\vec{n}-\vec{n}') = \sum_{\lambda\lambda'} c_2^0(\lambda) c_0^0(\lambda') \mathscr{V}_{\alpha i}(\vec{n},\lambda;\vec{n}',\lambda'), \tag{3.14}$$

with

$$\mathscr{V}_{\alpha i}(\vec{n},\lambda;\vec{n}',\lambda') = \frac{1}{\sqrt{4\pi}} \int d\Omega_\nu \int d\Omega_{\nu'} \times V_i(\vec{n},\lambda,\nu;\vec{n}',\lambda',\nu') S_2^\alpha(\Omega_\nu). \tag{3.15}$$

Here V_i is the derivative of $V(\vec{n},\lambda,\nu;\vec{n}',\lambda',\nu')$ with respect to $X_i(\vec{n}')$ taken at $\vec{s}=0$. Here again we restrict ourselves to nearest neighbors. The matrix elements $\mathscr{V}_{\alpha i}(\vec{n}-\vec{n}')$ depend on $\vec{X}(\vec{n}')-\vec{X}(\vec{n})$ and are discussed in Appendix B. V^{TR} can be considered as a special case of a crystal-field term in a deformed lattice. Since the lattice is deformed, the central molecule experiences no longer a cubic field but a deformed field. The SAF of the central molecule has then T_{2g} symmetry, while the surrounding molecules are still described by $S_{l=0}^{A_{1g}}$. For a review on T-R coupling we mention Ref. 10.

It is convenient to rewrite the interactions V^{RR} and V^{TR} in Fourier space. We write for the displacements

$$\vec{s}(\vec{n}) = (Nm)^{-1/2} \sum_{\vec{q}} \vec{s}(\vec{q}) e^{i\vec{q}\cdot\vec{X}(\vec{n})}, \tag{3.16}$$

where m is the molecular mass. Similarly we have for the orientational fluctuations

$$U_2^\alpha(\vec{n}) = N^{-1/2} \sum_{\vec{q}} U_2^\alpha(\vec{q}) e^{i\vec{q}\cdot\vec{X}(\vec{n})}. \tag{3.17}$$

The direct orientation-orientation interaction potential V^{RR} now reads

$$V^{RR} = \frac{1}{2} \sum_{\vec{q}} J^{\alpha\beta}(\vec{q}) U_2^\alpha(\vec{q}) U_2^\beta(-\vec{q}), \tag{3.18}$$

where the quadrupole-quadrupole interaction matrix is given by

$$J^{\alpha\beta}(\vec{q}) = \sum_{\vec{n}'} J^{\alpha\beta}(\vec{n}-\vec{n}') \exp[i\vec{q}\cdot\vec{X}(\vec{n}'-\vec{n})]. \tag{3.19}$$

We observe that here the word quadrupole refers to the fact that we describe the orientations by SAF's belonging to the manifold $l=2$, it is not restricted to the meaning of an electric quadrupole but also refers to the distribution of nuclear masses. Symmetry implies that the quadrupolar interaction becomes diagonal at the center of the Brillouin zone, where we write $J^{\alpha\beta}(\vec{q}=0) \equiv J_\Gamma \delta_{\alpha\beta}$. In Sec. V we will show that $J_\Gamma > 0$, which means that the direct rotational potential is repulsive at the Γ point. On the other hand, at the X point of the Brillouin zone, the interaction is again diagonal but its largest eigenvalue is negative: $J^{11}(\vec{q}_y^X) \equiv J_X^{11} < 0$, where $\vec{q}_y^X = (0, 2\pi/a, 0)$. We conclude that the direct quadrupolar interaction in solid C_{70} favors an antiferrorotational order with space group $Pa\bar{3}$. The situation is analogous to solid NaO_2. However while in the latter system a phase change $Fm\bar{3}m \rightarrow Pa\bar{3}$ takes place,[24] this is not the case for solid C_{70}. Indeed we will see that translation-rotation coupling always leads to an effective quadrupole-quadrupole interaction which is attractive at the Γ point. If this interaction is stronger than the direct interaction at the X point, the phase transition will be driven by the condensation of a zone-center mode, as is the case for $Fm\bar{3}m \rightarrow R\bar{3}m$.

The translation-rotation coupling is obtained as

$$V^{TR} = \sum_{\vec{q}} \mathscr{V}_{\alpha i}(\vec{q}) U_2^\alpha(-\vec{q}) s_i(\vec{q}). \tag{3.20}$$

In the limit of long wavelength, the coupling matrix reads

$$\mathscr{V}(\vec{q}) = \frac{2i\Lambda a}{\sqrt{m}} \begin{bmatrix} 0 & q_z & q_y \\ q_z & 0 & q_x \\ q_y & q_x & 0 \end{bmatrix}, \tag{3.21}$$

where a is the cubic lattice constant and Λ the T-R coupling constant. In Appendix B we show that Λ is a sum of matrix elements of type $\mathscr{V}_{\alpha i}(\vec{n}-\vec{n}')$, Eq. (3.14).

Finally we consider the elastic harmonic lattice potential

$$V^{TT} = \sum_{\vec{q}} \frac{1}{2} M_{ik}(\vec{q}) s_i(-\vec{q}) s_k(\vec{q}). \tag{3.22}$$

In the long-wavelength regime the dynamical matrix $M(\vec{q})$ is given by

$$M(\vec{q})=\frac{4a^3}{m}\begin{bmatrix} c_{11}^0 q_x^2+c_{44}^0(q_y^2+q_z^2) & d^0 q_x q_y & d^0 q_x q_z \\ d^0 q_y q_x & c_{11}^0 q_y^2+c_{44}^0(q_z^2+q_x^2) & d^0 q_y q_z \\ d^0 q_z q_x & d^0 q_z q_y & c_{11}^0 q_z^2+c_{44}^0(q_x^2+q_y^2) \end{bmatrix} \tag{3.23}$$

with $d^0 \equiv (c_{44}^0 + c_{12}^0)$, where c_{ij}^0 are the bare elastic constants.

The terms V^{TT} and V^{TR} give rise to an effective lattice-mediated interaction V_L^{RR}. For a given configuration of orientations $\{U_2^\alpha(\vec{q})\}$ we minimize V with respect to $s_i(\vec{q})$, eliminate the displacements and obtain

$$V_L^{RR} = -\sum_{\vec{q}} \frac{1}{2} C^{\alpha\beta}(\vec{q}) U_2^\alpha(-\vec{q}) U_2^\beta(\vec{q}), \tag{3.24}$$

where

$$C(\vec{q}) = \mathscr{V}(\vec{q}) M^{-1}(\vec{q}) \mathscr{V}^\dagger(\vec{q}) \tag{3.25}$$

represents the lattice-mediated orientational interaction.[14] Notice that this interaction depends on the direction of $\vec{q}$, in agreement with general properties of soft modes in cubic crystals.[25] The largest eigenvalue of $C(\vec{q})$ is given for $\vec{q}=(0,0,q_z)$ by

$$\lim_{q_z \to 0} C^{11}(\vec{q}) = 16 \frac{\Lambda^2}{a c_{44}^0} \equiv C_L . \tag{3.26}$$

As is well known, T-R coupling gives also rise to a self-interaction of each molecule with the deformed lattice. This interaction leads to a modification of the crystal field, where V^R is replaced by[26]

$$W^R = V^R + V^s . \tag{3.27}$$

The quantity V^s will be calculated in Appendix C.

IV. FREE ENERGY AND PHASE TRANSITION

A. Free energy

Starting from the orientation and translation-dependent interaction potential V, Eq. (3.5), and using the method of Ref. 17 we have derived the free energy as a functional of the instantaneous expectation values $U_2^{\alpha e}(\vec{q})$ and $s_i^e(\vec{q})$ of orientational and displacive order parameter variables. The phase transition from the cubic to the rhombohedral phase is driven by the condensation of the three components $U_2^{\alpha e}(\vec{q})$ of T_{2g} symmetry at the center of the Brillouin zone.[22,23,9] We then write

$$U_2^{\alpha e}(\vec{q}) = \sqrt{N}\eta^\alpha \delta_{\vec{q},0}, \tag{4.1}$$

where η^α is the order-parameter amplitude. There are four domains of the rhombohedral structure, depending on the alignment of the molecule along one of the four diagonals of the cube.[9] We choose the domain where the three components η^α are equal, and write $\eta^\alpha = \eta$, for $\alpha = 1,2,3$. Since the product of the three T_{2g} components of the order parameter is a cubic invariant, the free energy contains a third-order term and the phase transition will be of first order.[27]

In the long-wavelength limit it is convenient to use homogeneous strains ϵ which are defined by

$$\lim_{\vec{q}\to 0} i q_k s_j^e(\vec{q}) = \sqrt{mN}\,\epsilon_{kj} . \tag{4.2}$$

We then obtain for the Helmholz free energy

$$F = F_0 + F^{RR}[\eta] + F^{TR}[\eta,\epsilon] + F^{TT}[\epsilon]. \tag{4.3}$$

Here F_0 is the single molecule free energy. It will be of no relevance in the following.

The collective rotational free energy per molecule now reads

$$\frac{F^{RR}}{N} = A\eta^2 + B\eta^3 + C\eta^4, \tag{4.4}$$

where the coefficients A, B, and C are determined by the orientation and translation dependent interactions. In particular we have

$$A = \tfrac{3}{2}\,[(\chi_0)^{-1} + J_\Gamma + C^s], \tag{4.5}$$

where χ_0 is the single-particle orientational susceptibility

$$\chi_0^{\alpha\alpha} = T^{-1} Z_0^{-1}\ \mathrm{Tr}[(U^\alpha(\vec{n}))^2 \exp(-W^R/T)]. \tag{4.6}$$

Here the trace Tr stands for an integration over Euler angles, T is the temperature measured in energy units ($k_B = 1$) and W^R is the crystal-field potential (3.27).

Cubic symmetry implies that the matrix χ_0 is diagonal and that the elements are equal. We write χ_0 for χ_0^{11}. The same property holds for the interaction matrix, and in Eq. (4.5) J_Γ stands for J^{11} ($\vec{q}=0$). The quantity C^s in Eq. (4.5) denotes the self-interaction correction to the rotational interaction. It is given by[26]

$$C^s \vec{1} = \frac{1}{N} \sum_{\vec{q}} C(\vec{q}), \tag{4.7}$$

where the matrix $C(\vec{q})$ is defined by Eq. (3.25), while $\vec{1}$ is the 3×3 unit matrix. For the coefficients B and C we have obtained[20]

$$B = -T y_{123}^{(3)}, \tag{4.8}$$

$$C = \frac{T}{8}\,[2y_{1122}^{(4)} + y_{1111}^{(4)}]. \tag{4.9}$$

The quantities $y_{123}^{(3)}$, $y_{1122}^{(4)}$, and $y_{1111}^{(4)}$ are crystal-field thermal averages of three- and four-point rotator functions of T_{2g} symmetry. Analytical expressions are given in the second paper of Ref. 20.

The T-R coupling part of the free energy is given by

$$\frac{F^{TR}}{N} = 4a\Lambda(\epsilon_{yz} + \epsilon_{zx} + \epsilon_{xy})\eta, \tag{4.10}$$

a being the cubic lattice constant and where the coupling constant Λ has been introduced already in Eq. (3.21). Finally the elastic lattice energy in Eq. (4.3) is given by

$$\frac{F^{TT}}{N}=\frac{a^3}{8}[c_{11}^0(\epsilon_{xx}^2+\epsilon_{yy}^2+\epsilon_{zz}^2)+2c_{12}^0(\epsilon_{xx}\epsilon_{yy}+\epsilon_{yy}\epsilon_{zz}+\epsilon_{zz}\epsilon_{xx})+4c_{44}^0(\epsilon_{xy}^2+\epsilon_{yz}^2+\epsilon_{zx}^2)]. \quad (4.11)$$

Minimizing F with respect to ϵ_{ij} for fixed η, we obtain

$$\epsilon_{xy}=\epsilon_{yz}=\epsilon_{zx}=-\frac{4\Lambda}{a^2c_{44}^0}\eta. \quad (4.12)$$

Since the longitudinal strains do not couple to η, we put $\epsilon_{ii}=0$. Expression (4.12) will allow us to determine the magnitude and the sign of the shear strains.

B. Phase transition

We first have to evaluate the order parameter η. Eliminating the shear strains by means of Eq. (4.12) we obtain

$$F^{TT}+F^{TR}=-\tfrac{3}{2}C_L\eta^2, \quad (4.13)$$

where C_L is the lattice-mediated interaction constant, given by expression (3.26).

The bilinear coupling of elastic deformations to orientational order leads to a decrease of the free energy and hence to the stabilization of an ordered structure with a deformed unit cell. Combining Eqs. (4.13) and (4.4) we rewrite the free energy (4.3) as a Landau expansion

$$F=F_0+A'\eta^2+B\eta^3+C\eta^4, \quad (4.14)$$

where

$$A'=\tfrac{3}{2}[(\chi_0)^{-1}+J_\Gamma+C^s-C_L]. \quad (4.15)$$

As we have already seen in the last section, in absence of translation-rotation coupling, or equivalently of the lattice-mediated interaction, our model of solid C_{70} would lead to an antiferrorotational $Pa\bar{3}$ structure. In presence of T-R coupling, a ferroelastic transition to a $R\bar{3}m$ structure occurs under the condition that the lattice-mediated interaction is sufficiently large:

$$[C_L-J_\Gamma]>|J_X^{11}|. \quad (4.16)$$

The transition temperature of the first-order ferroelastic phase transition is given by

$$T_1=x^{(2)}(T_1)\left[C_L-C^s-J_\Gamma+\frac{B^2(T_1)}{6C(T_1)}\right]. \quad (4.17)$$

The discontinuity of the order parameter at the transition is obtained as[27]

$$\eta=\frac{-B(T_1)}{2C(T_1)}. \quad (4.18)$$

We will find $B(T_1)<0$, $C(T_1)>0$ and hence $\eta>0$.

Using methods of molecular field theory, we have calculated the collective orientational susceptibility in the disordered phase[17]

$$\chi(\vec{q})\equiv\langle\vec{U}_2(\vec{q})U_2(-\vec{q})\rangle/T=\chi_0[\vec{1}-\chi_0(C(\vec{q})-J(q)-\vec{1}C^s)]^{-1}. \quad (4.19)$$

The corresponding expression in the ordered phase is obtained by replacing χ_0 by χ_0-(η^2/T). As a consequence of bilinear T-R coupling, we get for the displacive susceptibility[14]

$$D^{-1}(\vec{q})\equiv\langle s(\vec{q})s(-\vec{q})\rangle/T=M^{-1}(\vec{q})[\vec{1}+\mathscr{T}^\dagger(\vec{q})\chi(\vec{q})\mathscr{T}(\vec{q})M^{-1}(\vec{q})], \quad (4.20)$$

and therefrom we deduce the shear elastic constant[26,10]

$$c_{44}=c_{44}^0\left\{\frac{T-x^{(2)}(T)[C_L-J_\Gamma-C^s]}{T+x^{(2)}(T)[C^s+J_\Gamma]}\right\}. \quad (4.21)$$

The increase of the orientational susceptibility near T_1 leads to a softening of c_{44}.

V. NUMERICAL RESULTS

In Sec. III we have shown how the intermolecular potential constants can be described on a microscopic scale by interactions between atomic centers (C), double-bonds centers (D), and intermediate centers (I) on different molecules. Since so far it is not possible to obtain these interactions from *ab initio* electronic-structure calculations, one has to resort to phenomenological considerations. As a guideline one takes the interatomic potentials of graphite. For the case of solid C_{60} this procedure has been taken as a starting point of molecular-dynamics simulations.[28] Interaction sites on short C-C bonds (D centers) had to be taken into account[29] in order to reproduce the right low-temperature structure ($Pa\bar{3}$). The consideration of D centers is also justified by the electronic structure of the molecule, since the π-electron clouds which contribute to the short C-C bonds extend radially outward from the bond.[30] The calculations of Refs. 28 and 29 have been based on (12-6) Lennard-Jones (LJ) potentials between these interaction centers. In addition Coulomb charges of opposite sign were put on C centers and on D centers, the total charge on the molecule being zero. These concepts were applied and extended for molecular-dynamics simulations on solid C_{70}, where in addition to C and D centers, I centers on intermediate bonds were considered.[2] In the present paper we use the same configuration of centers, however the interactions between centers are described by a sum of repulsive Born-Mayer (BM) potentials and attractive van der Waals (W) potentials:

$$V(\vec{n},\lambda,\nu;\vec{n}',\lambda',\nu')=C_{\lambda\lambda'}^{(1)}\exp(-C_{\lambda\lambda'}^{(2)}r)-B_{\lambda\lambda'}r^{-6}. \quad (5.1)$$

Here r is the distance between the centers $\nu(\lambda)$ and $\nu(\lambda')$ belonging to different molecules $\vec{n}$ and $\vec{n}'$ [see Eq. (3.4)]. The choice of an (Exp-6) potential has been motivated by our experience with the calculation of crystal-field coefficients $w_l^{A_{1g}}$ [see Eq. (3.10)] in solid C_{60}.[20,31,32] On the other hand, these coefficients have been deduced from single-crystal synchrotron radiation[33] and high-resolution neutron powder-diffraction experiments.[34] So a direct comparison be-

TABLE II. Interaction potential parameters between centers belonging to different molecules. The label λ is only relevant in as far as its specifies the type of center. $C^{(2)}_{\lambda\lambda'}$ in units Å^{-1}. $C^{(1)}_{\lambda\lambda'}=6.24\times10^6$ K, $B_{\lambda\lambda'}=4.24\times10^4$ K Å^6, irrespective of type.

Type	*C,C*	*D,D*	*C,D*	*I,I*	*C,I*	*D,I*
$C^{(2)}_{\lambda\lambda'}$	3.6	3.2	3.4	3.4	3.5	3.3

tween theory and experiment becomes possible for solid C_{60}. Theoretical calculations[31] show that the true values of $w_l^{A_{1g}}$ are the result of a subtle interplay between contributions from different types of centers. It is easier in our calculations to achieve agreement with experiment by using (Exp-6) potentials[32] rather than by using (12-6) potentials.[31] We have attributed this to the comparatively slower decay of BM potentials in comparison of repulsive (12) potentials with increasing distance [see discussion following Eq. (3.16) of Ref. 32].

(Exp-6) potentials for *C*-*C* interactions in solid C_{70} have been suggested in Ref. 35. For the present calculations we have chosen the potential parameter values which are quoted in Table II. Here $C^{(2)}_{CC}=3.6$ Å^{-1} is the value given in Refs. 35 and 36, while for $C^{(2)}_{DD}$, due to the extension of the π-electron cloud, we have chosen 3.2 Å^{-1}. For the *I* centers we have taken intermediate values. The constants $C^{(1)}_{\lambda\lambda'}$ and $B_{\lambda\lambda'}$ were taken to be the same for all type of centers, however their values are smaller than for a molecule which would only have *C* centers [a similar choice is also made for the (12-6) potential in C_{70} where the parameter ϵ has a reduced value[2]]. In contradistinction to molecular dynamics,[2] we have not taken into account Coulomb charges. In solid C_{60}, the electric multipoles turned out to be smaller[37] than originally anticipated. An electrical quadrupole moment would have influence on the transition temperature, since it contributes to the direct orientational interaction. It increases the value of J_Γ (repulsive at the Brillouin-zone center) and the absolute value of J_X^{11}, which favors a $Pa\bar{3}$ structure [see condition (4.16)]. In other words, while in solid C_{60} electrostatic interactions were found to increase the transition temperature,[29] they disfavor the ferroelastic transition in solid C_{70}. This may be the reason why, at short distances between *C* centers (say 2.5 Å), we can choose a BM potential that is weaker by a factor 0.37 in comparison with the repulsive part of the LJ potential of Ref. 2. A further reason why we favor smaller values for the repulsive potential at short distances is the fact that we have to calculate the convolution integrals (3.7), (3.12), and (3.15) on a rigid lattice at zero center-of-mass displacements, while in molecular-dynamics simulations the center-of-mass positions adjust themselves to the molecular orientations.

Starting from the potential (5.1) with parameters from Table II, using the molecular parameters from Table I and taking a cubic lattice constant $a=15$ Å, we have calculated by numerical integrations the coefficients $\mathscr{T}^{\alpha\beta}_{\lambda\lambda'}(\vec{n}-\vec{n}')$, Eq. (3.7). With the molecular structure coefficients $c^0_l(\lambda)$ from Table I we then obtain the direct quadrupolar interaction $J^{\alpha\beta}(\vec{n}-\vec{n}')$, Eq. (3.9a), and its Fourier transform $J(\vec{q})$, Eq. (3.19). In Table III we have quoted the contributions to $J_\Gamma\equiv J^{11}(\vec{q}=0)$ and $J_X^{11}\equiv J^{11}(\vec{q}_y^X)$ due to the different types of interaction centers λ, λ′. As we have anticipated in the previous section, we see from the last row in Table III ("sum") $J_\Gamma>0$ and $J_X^{11}<0$, which shows that the direct quadrupole-quadrupole interaction is antiferrorotational. The main contributions are due to *C* and *D* centers, while *I* centers, which are of minor importance, oppose the effect of *C* and *D* centers (different sign). In other words the contributions from *I* centers, which are attractive at the Γ point favor a ferrorotational phase transition. Within our calculations this effect can be understood as follows. *I* centers are on the average at shorter distance from the molecular center of mass (see Table I, column 7) of the molecule to which they belong. Hence their distances to *I*, *C* or *D* centers of a neighboring molecule are relatively large, and consequently the attractive van der Waals part of the potential (5.1) becomes comparable or even more important than the repulsive Born-Mayer part. On the other hand, for interactions where only *C* and *D* centers are involved, the repulsive BM part of the potential is dominant.

Further we have calculated numerically the coefficients $\mathscr{T}_{\alpha i}(\vec{n},\lambda;\vec{n}',\lambda')$, Eq. (3.15), of the *T*-*R* coupling interaction. Using Eq. (B7), we find the coupling constant Λ. In the fourth column of Table III we have quoted the contributions of different types of interaction centers to Λ. Notice that here again the major contributions are due to interactions involv-

TABLE III. Contributions from various centers to molecular interactions. Orientational interaction constants in units K. *T*-*R* coupling Λ in units K/Å.

λ,λ′	J_x^{11}	J_Γ	Λ	w_4	w_6	w_8
C,C	−2269.5	2115.7	−1006.3	−305.4	−353.6	67.1
C,D	−4255.6	3924.9	−1603.0	−152.3	1075.5	−620.4
D,D	−2147.8	1957.1	−641.2	68.9	849.1	−380.2
I,I	162.6	−75.3	10.6	11.3	2.2	−12.3
I,C	557.9	−647.9	−70.8	−75.5	−37.4	−42.9
I,D	759.3	−807.9	−39.3	−81.2	258.9	−364.9
Sum	−7193.0	6466.6	−3350.0	−535.4	1794.6	−1353.7

ing only C and D centers, while I centers act in the opposite sense. In order to calculate the lattice-mediated orientational interaction C_L, Eq. (3.26), and the self-interaction C^s, Eq. (4.7), we need the bare elastic constants c^0_{ij}. These are virtual quantities which refer to the crystal in absence of T-R coupling. In principle, it should be possible to calculate their values by using the methods of Sec. III. In a first attempt we did start from our intermolecular potentials with the nearest-neighbor interactions, calculated the second derivatives with respect to the displacements, and averaged over the orientations. Using these second-order lattice coupling constants, we have calculated the cubic elastic constants. We obtained values that are too small by one order of magnitude, the value of the lattice-mediated interaction C_L is then excessively large as is also the case for the transition temperature. We conclude that our calculation is oversimplified. Probably two extensions are necessary. First one should take into account further neighbor molecules, and secondly lattice anharmonicities are likely to be important. Such a calculation along the lines of a renormalized harmonic approximation is beyond the scope of the present work. Adopting a more pragmatic approach here, we assume that in absence of T-R coupling, solid C_{70} becomes similar to solid C_{60}. We then take as values of the elastic constants $c^0_{11}=2235$, $c^0_{12}=950$, and $c^0_{44}=875$, in units K/Å^3, close to the elastic constants of solid C_{60}.[38] With $\Lambda=-3350.2$ K/Å from Table III, we calculate the lattice-mediated orientational interaction by means of Eq. (3.26) and obtain $C_L=13\,678$ K. With the values $J_\Gamma=6466$ K and $J^{11}_X=-7193$ K, we see that condition (4.16) for the occurrence of a ferroelastic interaction is realized. It also follows from Table III that C,D and D,D interactions, since their negative contributions to J^{11}_X are large, favor an antiferrorotational $Pa\bar{3}$ structure. In this respect we recall that in solid C_{60}, as has been shown by molecular-dynamics simulations,[29] D centers are indeed necessary for the stabilization of the $Pa\bar{3}$ structure. In solid C_{70}, the large value of the lattice-mediated interaction C_L is ultimately responsible for the transition to the $R\bar{3}m$ structure. Notice however that without interactions involving D centers, it would be much easier to satisfy condition (4.16). Our expression (3.26) of C_L shows that it is advantageous for the occurrence of a ferroelastic transition that c^0_{44} is small. However from Eq. (4.17) we also see that a large value of C_L leads to a large value of the transition temperature T_1. The used values of the elastic constants allow us to satisfy two opposing requirements: condition (4.16) on one hand, and a sufficiently low value of T_1 on the other hand.

The self-interaction C^s is obtained from Eq. (4.7), where we calculate numerically the integral over the Brillouin zone. We obtain $C^s=5350$ K for the case of T_{2g} symmetry and $C^s=507$ K for the case of E_g symmetry.

Next we turn to the evaluation of the crystal field, Eq. (3.27), where V^R is the crystal field in the rigid lattice and where V^s is due to the self-interaction in the deformable lattice. The coefficients $w^{A_{1g}}_l$ in expression (3.10) are calculated by means of Eqs. (3.11) and (3.12). The results are quoted in Table III, where we have again shown the contributions from various types of interaction centers. Inspection of the results show that, even within a same manifold l, contributions from C,C, C,D, and D,D interactions have not the same sign. This subtle fact is due to the *linear* dependence of $w^{A_{1g}}_l$, Eq. (3.11), on the structure constants $c^0_l(\lambda)$, $l\neq 0$. The sign of these structure constants (see Table I) is specific for the location of a center on the molecule. In other words the crystal-field coefficients reflect in a rather direct way the electronic structure of the molecule. This fact has been discussed before[31] in the case of solid C_{60}. There it has also been shown that the crystal-field coefficients can be obtained from diffraction experiments.[33,34] For the case of C_{70} we see from Table III that the presence of double-bond interaction centers is responsible for the large positive value of $w^{A_{1g}}_6$. In particular we find that the matrix elements $\mathscr{V}^{A_{1g}}_l(\lambda,\lambda')$ where D centers are involved are negative, while from Table I we see that $c^0_6(6)=-2.84$. Using expression (3.11) and observing that $c^0_0(\lambda)>0$, we obtain the positive contributions from C,D and D,D interactions to $w^{A_{1g}}_6$. Notice that, since $c^0_6(7)=0.61$, the D centers with label $\lambda=7$ yield negative contributions to $w^{A_{1g}}_6$, however since $d(7)<d(6)$, the matrix elements are smaller than those of centers with label $\lambda=6$.

The self-interaction V^s leads to a replacement of $w^{A_{1g}}_4=-534.4$ K by $\tilde{w}^{A_{1g}}_4=1354.4$ K, as is shown in Appendix C. The crystal field W^R now reads

$$W^R=\sum_{\vec{n}}\left[\tilde{w}^{A_{1g}}_4 U^{A_{1g}}_4(\vec{n})+w^{A_{1g}}_6 U^{A_{1g}}_6(\vec{n})+w^{A_{1g}}_8 U^{A_{1g}}_8(\vec{n})\right]. \tag{5.2}$$

This expression is used for the calculation of single-particle thermal averages $\langle\ \rangle_R$ in the quantities χ_0, B, and C of Sec. IV. The integrations over Euler angles are done numerically. At the end of this section we will show how the crystal-field coefficients affect the orientational density distribution.

Starting from the results of Sec. IV and using the numerical information from Table III, we have calculated various physical quantities. From Eq. (4.17) we find that our model of solid C_{70} exhibits a first-order phase transition at $T_1=462$ K, and that the virtual second-order transition is at $T_c=457$ K. The discontinuity of the order parameter at T_1 is obtained from Eq. (4.28) and we find $\eta=0.08$. Since we obtain $\eta>0$, and since $\Lambda<0$, it follows from Eq. (4.12) that the shears ϵ_{ij} are positive. The positive values of the shears corresponds to a stretching of the unit cell along the former cubic direction [111], as is experimentally observed[6,3,8] and obtained from molecular-dynamics simulations.[2]

Next we have calculated the collective orientational susceptibility $\chi(\vec{q})$ given by Eq. (4.19). The temperature evolution of $\chi^{11}(\vec{q})$ for $\vec{q}=(0,0,q_z)$ is shown in Fig. 1. The temperature dependence of the shear elastic constant c_{44}, calculated from Eq. (4.21), is shown in Fig. 2. The softening of the elastic constant c_{44} at the phase transition is a consequence of T-R coupling (see Ref. 10 for a review). So far we know only about measurements of elastic constants in hexagonal crystals,[39] where anomalies are found at successive phase transitions. We encourage and look forward to experiments in fcc crystals.

Knowledge of the crystal field allows us to determine the orientational density distribution[40] of a molecule in the disordered phase. We will restrict us to the ten nuclei located on the two pentagons on the outer caps of the molecule. These

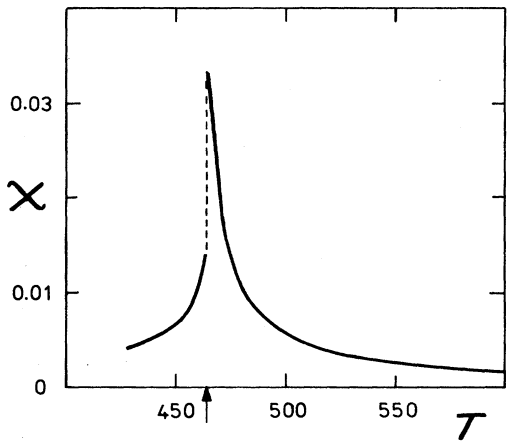

FIG. 1. Collective orientational susceptibility, units K^{-1}. Arrow indicates transition temperature. The dashed line indicates discontinuity at the first-order phase transition.

nuclei belong to the group of centers $\lambda=5$. Proceeding as in Ref. 41, we obtain for the orientational density distribution

$$f(\Omega)=\sum_l \gamma_l^{A_{1g}} K_l^{A_{1g}}(\Omega). \tag{5.3}$$

Here $K_l^{A_{1g}} \equiv S_l^{A_{1g}}$ are the cubic harmonics[42] of symmetry O_h, and the coefficients $\gamma_l^{A_{1g}}$ are thermal averages over the orientational motion

$$\gamma_l^{A_{1g}} = c_l^0(\lambda=5)\langle U_l^{A_{1g}}\rangle_R . \tag{5.4}$$

The functions $U_l^{A_{1g}}$ are defined by Eq. (A10), and the coefficients $c_l^0(5)$ are quoted in Table I. We observe that for $l=0$, $c_0^0(5)=10/\sqrt{4\pi}$. We have calculated numerically the thermal averages $\langle U_l^{A_{1g}}\rangle_R$, using the crystal field W^R. Taking $T=500$ K, we obtain $\gamma_l^{A_{1g}}=-0.859$, -0.856, and -0.1936, for $l=4$, 6, and 8, respectively. In Fig. 3 we present a plot of $f(\Omega)$ in a (110) plane in the disordered phase. The distribution exhibits sharp maxima in $\langle 110\rangle$ directions. These

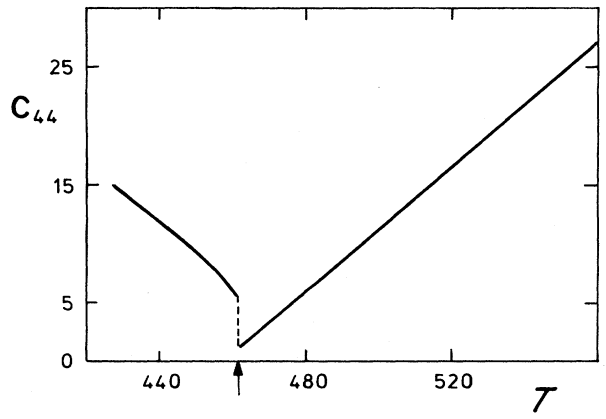

FIG. 2. Temperature evolution of elastic constant c_{44}, units K/Å^3. Arrow indicates the transition temperature.

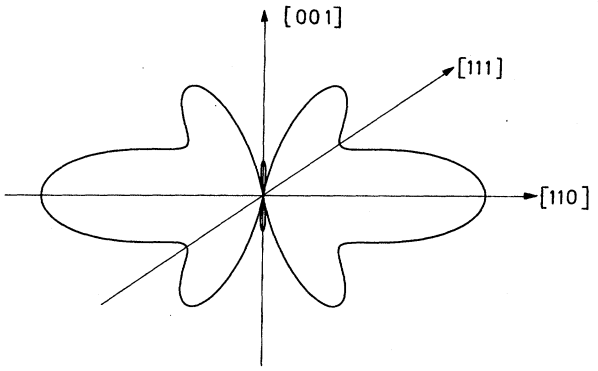

FIG. 3. Orientational distribution function of long molecular axis in (110) plane, disordered phase. Numbers within square brackets indicate directions in cubic crystal.

maxima are a consequence of the large positive value of the crystal-field coefficients. In particular a positive value of $w_4^{A_{1g}}$ pushes the molecule away from $\langle 100\rangle$ and a positive value of $w_6^{A_{1g}}$ is strongly repulsive for $\langle 111\rangle$. The preferential orientation of the molecule along $\langle 110\rangle$ is in agreement with molecular-dynamics simulations[2] and with NMR line-shape data.[43] Our calculations show that the large positive value of $w_6^{A_{1g}}$ is a consequence of the double bond (D) interaction centers. Without D centers, $w_6^{A_{1g}}$ would be negative and favor an orientation along $\langle 111\rangle$ in the disordered phase. Similar conclusions have been reached by molecular dynamics.[2] We see that the orientational distribution of the molecule in the disordered phase reflects the electronic structure of the molecule.

VI. CONCLUDING REMARKS

Starting from a phenomenological model of the intermolecular potential,[2] which is based on interactions between atomic (C), double bond (D), and intermediate (I) centers of neighboring molecules, we have developed a theory of the orientational phase transition $Fm\bar{3}m \rightarrow R\bar{3}m$ in solid C_{70}. We have shown that the bilinear T-R coupling leads to a lattice-mediated orientational interaction which is maximum and attractive at the center of the Brillouin zone. We have carried out quantitative calculations and found that the lattice-mediated interaction overcomes the influence of the direct orientational interaction, which would favor an antiferrorotational order of symmetry $Pa\bar{3}$, as is the case for solid C_{60}. We have calculated the discontinuity of the orientational order parameter at the ferroelastic phase transition and find that the concomitant lattice shears are positive, which corresponds to a stretching of the primitive unit cell along a cubic [111] direction. We have also studied the temperature evolution of the collective orientational susceptibility and the related softening of the elastic constant c_{44} near the phase transition. Finally we have investigated the orientational distribution function of a C_{70} molecule in the orientationally disordered phase. We find that $\langle 110\rangle$ are directions of preferential orientations. We have shown that the orientational distribution reflects the electronic structure of the molecule, in

particular the importance of the double bonds. The important achievement is that the theory describes a range of experimental facts in a qualitative correct way. In order to gain additional information about the intermolecular potential in solid C_{70}, it would be very useful to perform diffraction experiments, similar to those which have been carried out[33,34] in solid C_{60}.

The ferroelastic phase transitions in solid C_{70} are to a large extent similar to those encountered in the alkalicyanides or mixed alkalicyanides halides.[11,22] Hence it is not surprising that solid C_{70} exhibits pronounced thermal hysteresis effects.[6,44,45]

ACKNOWLEDGMENT

This work was financially supported by the Science Foundation of Belgium.

APPENDIX A

Here we give explicitly the relevant site symmetry adapted functions $S^{\tau}_{l(O_h)}$ and the corresponding rotator functions. Following Ref. 21, we define

$$Y_l^{m,c}=(Y_l^m+Y_l^{-m})/\sqrt{2}, \tag{A1}$$

$$Y_l^{m,s}=-i(Y_l^m-Y_l^{-m})/\sqrt{2}. \tag{A2}$$

For the manifold $l=2$, we have only one representation $\Gamma=T_{2g}$. The corresponding three basis functions which we denote by S_2^{α} are given by[21]

$$S_2^{\alpha=1}\equiv Y_2^{1,s};\quad S_2^{\alpha=2}\equiv Y_2^{1,c};\quad S_2^{\alpha=3}\equiv Y_2^{2,s}. \tag{A3}$$

Here Y_l^m stands for $Y_l^m(\Omega)$. Defining $x=\sin\theta\cos\phi$, $y=\sin\theta\sin\phi$, $z=\cos\theta$, and making use of Eq. (2.2), we find that the functions S_2^{α} are equal to yz,zx,xy for $\alpha=1,2,3$, respectively. Using Eqs. (2.8) and (3.8), we obtain the rotator functions

$$U_2^{\alpha=1}(\omega)=\sqrt{4\pi/5}Y^{1,s}(\beta,\alpha), \tag{A4}$$

$$U_2^{\alpha=2}(\omega)=-\sqrt{4\pi/5}Y_2^{1,c}(\beta,\alpha), \tag{A5}$$

$$U_2^{\alpha=3}(\omega)=-\sqrt{4\pi/5}Y_2^{2,s}(\beta,\alpha). \tag{A6}$$

The functions of A_{1g} symmetry are also tabulated in Ref. 21. They belong to the manifolds $l=4,6,8,\ldots$. Explicitly

$$S_4^{A_{1g}}=0.7638Y_4^0+0.6455Y_4^{4,c}, \tag{A7}$$

$$S_6^{A_{1g}}=0.3536Y_6^0-0.9354Y_6^{4,c}, \tag{A8}$$

$$S_8^{A_{1g}}=0.7181Y_8^0+0.38188Y_8^{4,c}+0.5818Y_8^{8,c}. \tag{A9}$$

The corresponding rotator functions (3.8) are then given by

$$U_l^{A_{1g}}(\omega)=\sqrt{4\pi/(2l+1)}S_l^{A_{1g}}(\beta,\alpha). \tag{A10}$$

We observe that these rotator functions are normalized such that

$$\int d\omega\ U_l^{1\tau}(\omega)U_{l'}^{1\tau'}(\omega)=\frac{8\pi^2}{2l+1}\delta_{ll'}\delta_{\tau\tau'}. \tag{A11}$$

Here $d\omega=d\alpha\ d\gamma\sin\beta d\beta$, with $0\leq\alpha\leq2\pi$, $0\leq\gamma\leq2\pi$, $0\leq\beta\leq\pi$.

Finally we quote the site symmetry adapted functions for E_g symmetry. There are two functions belonging to the manifold $l=2$. From Ref. 21 we have

$$S_2^{\alpha=1,E}\equiv Y_2^0;\quad S_2^{\alpha=2,E}\equiv Y_2^{2,c}, \tag{A12}$$

and for the rotator functions we get

$$U_2^{\alpha=1,E}(\omega)=\sqrt{4\pi/5}Y_2^0(\beta,\alpha), \tag{A13}$$

$$U_2^{\alpha=2,E}(\omega)=\sqrt{4\pi/5}Y_2^{2,e}(\beta,\alpha). \tag{A14}$$

APPENDIX B

Here we will give additional details on the T-R coupling. The Fourier transformed interaction is defined as

$$\mathscr{V}_{\alpha i}(\vec{q})=\sum_{\vec{n}'}\mathscr{V}_{\alpha i}(\vec{n}-\vec{n}')\exp[i\vec{q}\cdot\vec{X}(\vec{n}'-\vec{n})]. \tag{B1}$$

We will restrict ourselves to the 12 nearest neighbors $\vec{n}'$ of $\vec{n}$ on the fcc lattice and write $\mathscr{V}_{\alpha i}(\vec{\kappa})$ for $\mathscr{V}_{\alpha i}(\vec{n}-\vec{n}')$, with $\vec{\kappa}=1-12$. In order to study the structure of this interaction in real space, we consider first the situation where the central molecule at $\vec{n}$ is surrounded by the four molecules in the (001) plane, i.e., with neighbors at points $(\pm a/2,\pm a/2,0)$ relative to (0,0,0). Taking into account Eqs. (3.15) and (3.13), we calculate the matrix elements $\mathscr{V}_{\alpha i}(\vec{\kappa})$, for $\vec{\kappa}=1-4$, where $\vec{\kappa}=1$ refers to $\vec{n}'$ at $(a/2,a/2,0)$, etc. We obtain

$$[\mathscr{V}_{\alpha i}(1)]=\begin{pmatrix}0&0&A_2\\0&0&A_2\\B_2&B_2&0\end{pmatrix}. \tag{B2}$$

For $\kappa=2$, $\vec{n}'$ at $(-a/2,a/2,0)$, we get

$$[\mathscr{V}_{\alpha i}(2)]=\begin{pmatrix}0&0&A_2\\0&0&-A_2\\B_2&-B_2&0\end{pmatrix}. \tag{B3}$$

For $\kappa=3$, $\vec{n}'$ at $(-a/2,-a/2,0)$, we get

$$[\mathscr{V}_{\alpha i}(3)]=-[\mathscr{V}_{\alpha i}(1)], \tag{B4}$$

and for $\vec{\kappa}=4$, $\vec{n}'$ at $(a/2,-a/2,0)$, we find

$$[\mathscr{V}_{\alpha i}(4)]=-[\mathscr{V}_{\alpha i}(2)]. \tag{B5}$$

Similar relations hold for the molecules $\vec{\kappa}=5-8$ in the (100) plane and $\vec{\kappa}=9-12$ in the (010) plane. The corresponding matrices are easily obtained by symmetry considerations from expressions (B2)–(B5). Defining $\vec{X}(\vec{\kappa})=\vec{X}(\vec{n}')-\vec{X}(\vec{n})$, and using symmetry relations we rewrite expression (B1) as

$$\mathscr{V}_{\alpha i}(\vec{q})=i\sum_{\vec{\kappa}=1}^{12}\mathscr{V}_{\alpha i}(\vec{\kappa})\sin[\vec{q}\cdot\vec{X}(\vec{\kappa})]. \tag{B6}$$

In the long-wavelength limit, expression (B6) reduces to Eq. (3.20), where

$$\Lambda=A_2+B_2. \tag{B7}$$

With the potential parameters of Table II, we find $\Lambda=-3350$ K/Å.

We have also calculated the T-R coupling for the case of orientational fluctuations of E_g symmetry belonging to the manifold $l=2$. The coupling matrix is given by

$$\mathscr{T}^{E_g}(\vec{q})=\frac{2i\Lambda^{E_g}a}{\sqrt{m}}\begin{bmatrix} q_x & q_y & -2q_z \\ -\sqrt{3}q_x & \sqrt{3}q_y & 0 \end{bmatrix}. \quad \text{(B8)}$$

We have evaluated Λ^{E_g} with the potential parameters of Table II and obtain $\Lambda^{E_g}=867$ K/Å. Consequently the lattice-mediated interaction for E_g fluctuations is an order of magnitude smaller than for T_{2g} fluctuations. For the corresponding self-interaction we calculate the value $C^{sE_g}=507$ K.

APPENDIX C

Here we study the effect of the self-interaction on the crystal field. It has been shown previously[17,26] that the contribution V^s in Eq. (3.27) is given by

$$V^s=-\frac{1}{2}\sum_{\vec{n}}\sum_{\tau} C^{s,\tau}[U_2^{1\tau}(\vec{n})]^2. \quad \text{(C1)}$$

Here we restrict ourselves to contributions belonging to the manifold $l=2$, the index $\tau=(\Gamma,\alpha)$ labels the representations $\Gamma=T_{2g}$ and E_g, and α labels the components 1–3 and 1,2, respectively. As a consequence of the generalized Unsöld theorem[46] we have

$$-\sum_{\alpha=1}^{3}(S_2^{\alpha,T_{2g}})^2=\sum_{\alpha=1}^{2}(S_2^{\alpha,E_g})^2=\sqrt{3/7\,\pi}S_4^{A_{1g}}. \quad \text{(C2)}$$

Using the relations between the rotator functions and the surface harmonics, Eqs. (A4)–(A6), Eqs. (A13), (A14), and (A10), we rewrite expression (C1) as

$$V^s=\alpha_4^{A_{1g}}\sum_{\vec{n}} U_4^{1A_{1g}}(\vec{n}), \quad \text{(C3)}$$

where

$$\alpha_4^{A_{1g}}=0.39(C^{s,T_{2g}}-C^{s,E_g}). \quad \text{(C4)}$$

With the values $C^{s,T_{2g}}\equiv C^s=5350$ K, $C^{s,E_g}=507$ K, we obtain $\alpha_4^{A_{1g}}=1889$ K, and consequently, since $w_4^{A_{1g}}=-534.4$ K,

$$\tilde{w}_4^{A_{1g}}=w_4^{A_{1g}}+\alpha_4^{A_{1g}} \quad \text{(C5)}$$

is equal to 1354.4 K.

[1] G. B. M. Vaughan, P. A. Heiney, J. E. Fischer, D. E. Luzzi, D. A. Ricketts-Foot, A. R. McGhie, Y. W. Hui, A. L. Smith, D. E. Cox, W. J. Romanov, B. H. Allen, N. Coustel, J. P. McCauley, Jr., and A. B. Smith, III, Science **254**, 1350 (1992).

[2] M. Sprik, A. Cheng, and M. L. Klein, Phys. Rev. Lett. **69**, 1660 (1992).

[3] C. Christides, I. M. Thomas, T. J. S. Dennis, and K. Prassides, Europhys. Lett. **22**, 611 (1993).

[4] K. Prassides, H. W. Kroto, R. Taylor, D. R. M. Walton, W. I. F. David, J. Tomkinson, R. C. Haddon, M. J. Rosseinsky, and D. W. Murphy, Carbon **30**, 1277 (1992).

[5] J. D. Axe, S. C. Moss, and D. A. Neumann, in *Solid State Physics: Advances in Research and Applications*, edited by H. E. Ehrenreich and F. Spaepen (Academic, New York, 1994), Vol. 48, p. 149.

[6] G. Van Tendeloo, S. Amelinckx, J. L. de Boer, S. van Smaalen, M. A. Verheijen, H. Meekes, and G. Meijer, Europhys. Lett. **21**, 329 (1993).

[7] C. Christides, T. J. S. Dennis, K. Prassides, R. L. Cappelletti, D. A. Neumann, and J. R. D. Copley, Phys. Rev. B **49**, 2897 (1994).

[8] G. B. M. Vaughan, P. A. Heiney, D. E. Cox, J. E. Fischer, A. R. McGhie, A. L. Smith, R. M. Strongin, M. A. Cichy, and A. B. Smith, III, Chem. Phys. **178**, 599 (1993).

[9] R. Sachidanandam and A. B. Harris, Phys. Rev. B **49**, 2878 (1994).

[10] R. M. Lynden-Bell and K. H. Michel, Rev. Mod. Phys. **66**, 721 (1994).

[11] F. Lüty, in *Defects in Insulating Crystals*, edited by V. M. Tuchkevich and K. K. Shvarts (Springer-Verlag, Heidelberg, 1981), p. 69; J. Ortiz-Lopez and F. Luty, Phys. Rev. B **37**, 5443 (1988); **37**, 5452 (1988).

[12] K. Knorr and A. Loidl, Phys. Rev. B **31**, 5387 (1985); S. Elschner, K. Knorr, and A. Loidl, Z. Phys. B **61**, 209 (1985).

[13] J. M. Rowe, J. J. Rush, and S. Susman, Phys. Rev. B **28**, 3506 (1983); J. M. Rowe, J. Bouillot, J. J. Rush, and F. Lüty, Physica B **136**, 498 (1986).

[14] K. H. Michel and J. Naudts, Phys. Rev. Lett. **39**, 212 (1977); S. D. Mahanti and D. Sahu, *ibid.* **48**, 936 (1982).

[15] H. M. James and T. A. Keenan, J. Chem. Phys. **31**, 12 (1959).

[16] M. Yvinec and R. M. Pick, J. Phys. (Paris) **41**, 1045 (1980).

[17] K. H. Michel and K. Parlinski, Phys. Rev. B **31**, 1823 (1985).

[18] J. Baker, P. W. Fowler, P. Lazzeretti, M. Malagoli, and R. Zanasi, Chem. Phys. Lett. **184**, 182 (1991).

[19] R. Renker, F. Gompf, R. Heid, P. Adelmann, A. Heiming, W. Reichardt, G. Roth, H. Schober, and H. Rietschel, Z. Phys. B **90**, 325 (1993).

[20] K. H. Michel, J. R. D. Copley, and D. A. Neumann, Phys. Rev. Lett. **68**, 2929 (1992); K. H. Michel, Z. Phys. B **88**, 71 (1992).

[21] C. J. Bradley and A. P. Cracknell, *The Mathematical Theory of Symmetry in Solids* (Clarendon, Oxford, 1972).

[22] J.-C. Tolédano and P. Tolédano, Phys. Rev. B **21**, 1139 (1980).

[23] K. H. Michel and T. Theuns, Phys. Rev. B **40**, 5761 (1989).

[24] S. D. Mahanti and G. Kemeny, Phys. Rev. B **20**, 2105 (1979); P. Zielinski and K. Parlinski, J. Phys. C **17**, 3301 (1984).

[25] R. A. Cowley, Phys. Rev. B **13**, 4877 (1976); R. Folk, H. Iro, and F. Schwabl, Z. Phys. B **25**, 69 (1976); B. De Raedt, K. Binder, and K. H. Michel, J. Chem. Phys. **75**, 2977 (1981).

[26] K. H. Michel and J. M. Rowe, Phys. Rev. B **32**, 5818 (1985); **32**, 5827 (1985).

[27] L. D. Landau, Phys. Z. Sowjetunion **11**, 26, 545 (1937).

[28] A. Cheng and M. L. Klein, Phys. Rev. B **45**, 1889 (1992).

[29] M. Sprik, A. Cheng, and M. L. Klein, J. Phys. Chem. **96**, 2027 (1992).

[30] W. Krätschmer, L. D. Lamb, K. Fostiropoulos, and D. R. Huffman, Nature (London) **347**, 354 (1990).
[31] K. H. Michel, J. Chem. Phys. **97**, 5155 (1992); D. Lamoen and K. H. Michel, Z. Phys. B **92**, 323 (1993).
[32] D. Lamoen and K. H. Michel, J. Chem. Phys. **101**, 1435 (1994).
[33] P. C. Chow, X. Jiang, G. Reiter, P. Wochner, S. C. Moss, J. D. Axe, J. C. Hanson, R. K. McMullan, R. L. Meng, and C. W. Chu, Phys. Rev. Lett. **69**, 2943 (1992).
[34] W. I. F. David, R. M. Ibberson, and T. Matsuo, Proc. R. Soc. London Ser. A **442**, 129 (1993).
[35] B. J. Nelissen, P. H. M. van Loosdrecht, M. A. Verheijen, A. van der Avoird, and G. Meijer, Chem. Phys. Lett. **207**, 343 (1993).
[36] D. E. Williams, J. Chem. Phys. **47**, 4680 (1967).
[37] T. Yildirim, A. B. Harris, S. C. Erwin, and M. R. Pederson, Phys. Rev. B **48**, 1888 (1993); P. W. Fowler (private communication).
[38] J. Yu, L. Bi, R. Kalia, and P. Vashishta, Phys. Rev. B **49**, 5008 (1994).
[39] P. Dolinar, W. Schranz, A. Fuith, H. Warhanek, M. Haluska, and H. Kuzmany, Solid State Commun. **90**, 659 (1994).
[40] W. Press and A. Hüller, Acta Crystallogr. A **29**, 252 (1973).
[41] J. R. D. Copley and K. H. Michel, J. Phys. Condens. Matter **5**, 4353 (1993).
[42] F. C. von der Lage and H. Bethe, Phys. Rev. **71**, 617 (1947).
[43] R. Blinc, J. Dolinsek, J. Seliger, and D. Arcon, Solid State Commun. **88**, 9 (1993).
[44] A. R. McGhie, J. E. Fischer, P. W. Stephens, R. L. Cappelletti, D. A. Neumann, W. H. Mueller, H. Mohn, and H.-U. ter Meer, Phys. Rev. B **49**, 12 614 (1994).
[45] C. Meingast, F. Gugenberger, G. Roth, M. Haluska, and H. Kuzmany, Z. Phys. B **95**, 67 (1994).
[46] See, e.g., M. Tinkham, *Group Theory and Quantum Mechanics* (McGraw-Hill, New York, 1964), p. 81.